

# Articles

## Solvent Effect on Stress Relaxation of PET Filament Fibers and Self Diffusion of Crystallites

Nam Jeong Kim, Eung Ryul Kim, and Sang Joon Hahn\*

Department of Chemistry, Hanyang University, Seoul 133-791

Received September 19, 1990

Viscoelastic properties of PET filament fibers on stress relaxation were investigated in the solvents of H<sub>2</sub>O, 0.05% NaOH and 50% DMF using an Instron (UTM-4-100 Tensilon) with solvent chamber. The theoretical stress relaxation equation derived by applying the Ree-Eyring's hyperbolic sine law to dashpot of three element non-Newtonian model was applied to the experimental stress relaxation curves, and the model parameters  $G_1$ ,  $G_2$ ,  $\alpha$  and  $\beta$  were obtained. By analyzing temperature dependency of the relaxation time, the values of activation entropy, activation enthalpy and activation free energy for flow in PET filament fiber were evaluated, the activation free energy being about 25.7 kcal/mol. The self diffusion coefficient and hole distance were obtained from parameters  $\alpha$ ,  $\beta$  and crystallite size in order to study the self diffusion and the orientation of crystallites in amorphous region and the effect of solvent.

### Introduction

Three element non-Newtonian model<sup>1</sup> consisted of a spring and a Maxwell element in parallel was used to investigate the molecular structure and the mechanical properties of nonlinear viscoelastic polymeric materials. In this model, the springs follow Hook's law, and the dashpot follows Ree-Eyring's hyperbolic sine law<sup>2</sup> of plastic flow.

The stress relaxation at constant strain is caused by the flow process of the flow segments in the materials. The stress relaxation for high polymeric materials have been reported by following researchers. Meredith<sup>3</sup> described an experimental procedure for investigating stress relaxation. Ree and Hahn<sup>4</sup> applied a generalized equilibration theory of transient phenomena to the stress relaxation in wool fibers and polyisobutylene rings stretched at constant elongation. Hawthorne<sup>5</sup> studied the stress relaxation behavior of biaxially oriented semicrystalline PET by thermodynamical analysis. Meredith and Hsu<sup>6</sup> studied the stress relaxation of polyester and nylon fibers at a range of temperature and humidities. Passaglia and Koppehele<sup>7</sup> carried out researches on the relation between strain and stress relaxation.

However, the theoretical and phenomenological analyses for stress relaxation processes have not been performed sufficiently, due to the effect of crystallites on the relaxation of molecular segments in the amorphous region.

In this paper, the theoretical stress relaxation equation has been derived by applying the Ree-Eyring's hyperbolic sine law to dashpot of three element non-Newtonian model, and applied to the experimental data of PET filament fibers, and the spring constants and flow parameters involved in this equation were evaluated. We found that the variation of parameters with temperature and solvents on stress relaxation of PET filament fibers is related to crystallinity<sup>8</sup>, orientation<sup>9</sup>, self diffusion<sup>10</sup> of crystallites in amorphous region and effect of solvents. For a more detailed analysis, we detected even

slight changes in the stress relaxation behavior with respect to temperature and solvents.

### Theory

The deformation of polymeric materials involves flow units slipping over one another from one equilibrium position to another. Even when no external forces are acting, the same processes are going on due to thermal energy. This phenomenon is the self diffusion of flow segments and molecules in a polymeric material. Molecules and flow segments cannot move into the space occupied by another. As the result, all movements take place at loose or empty place called hole distance in the structure.

According to Eyring's rate theory of flow, strain rate  $dS/dt$  is given by the following equation<sup>2</sup>:

$$\frac{dS}{dt} = \frac{2\lambda k'}{\lambda_1} \sin h \frac{\lambda \lambda_2 \lambda_3}{2kT} f \quad (1)$$

Here,  $\lambda$  is the hole distance swept out by the motion of molecules and flow units. Consider two layers of flow segments in a solid, at a distance  $\lambda_1$  apart, and suppose that one flow unit slides past the other under the influence of an applied stress  $f$ .  $\lambda_2 \lambda_3$  is the effective cross sectional area of the flow segment normal to the direction of flow. Now by the statistical thermodynamic theory of reaction rates

$$k' = \left( \frac{kT}{h} \right) \exp \left( \frac{-\Delta G^*}{RT} \right) \quad (2)$$

so the strain rate becomes

$$\frac{dS}{dt} = \left( \frac{2\lambda kT}{\lambda_1 h} \right) \exp \left( \frac{-\Delta G^*}{RT} \right) \sin h \frac{\lambda \lambda_2 \lambda_3}{2kT} f \quad (3)$$

Eq. (3) is transformed into the following simple form:

$$\frac{dS}{dt} = \frac{1}{\beta} \sin h \alpha f \quad (4)$$

The quantity,  $\beta$ , is called the relaxation time, and  $1/\alpha$  is proportional to the intrinsic strain modulus. This Ree-Eyring's non-Newtonian flow equation was applied to the dashpot of the three element non-Newtonian model.

For the non-Newtonian Maxwell element of model with a spring of modulus  $G_1$  and stress  $f_1$ , we have:

$$\frac{dS}{dt} = \frac{1}{G_1} \frac{df_1}{dt} + \frac{1}{\beta} \sin h \alpha f_1 \quad (5)$$

For the parallel spring of stress  $f_2$ , so that strain rate

$$\frac{dS}{dt} = \frac{1}{G_2} \frac{df_2}{dt} \quad (6)$$

The total stress  $f_T$  is the sum of all the partial stresses, therefore:

$$\frac{df_T}{dt} = \frac{df_1}{dt} + \frac{df_2}{dt} \quad (7)$$

From Eq. (5), (6), (7), we have:

$$\frac{df_T}{dt} = (G_1 + G_2) \frac{dS}{dt} - \frac{G_1}{\beta} \sin h \alpha (f_T - G_2 S) \quad (8)$$

For the stress relaxation with constant strain  $S_c$ , we have  $\frac{dS}{dt} = 0$ , and Eq. (8) become

$$\frac{df_T}{dt} = \frac{G_1}{\beta} \sin h \alpha (f_T - G_2 S_c) \quad (9)$$

from which:

$$\frac{df_T}{\sin h \alpha (f_T - G_2 S_c)} = -\frac{G_1}{\beta} dt \quad (10)$$

On integration, this gives:

$$\ln \tan h \alpha [(f_T - G_2 S_c)/2] = -G_1 \left( \frac{1}{\beta} \right) t + c \quad (11)$$

As boundary conditions, initial stress  $f_0 = (G_1 + G_2) S_c$  at  $t=0$ , and final stress  $f_\infty = G_2 S_c$  at  $t=\infty$  can be applied since the stress on Maxwell element decays very slowly.

Integral Constant is given by boundary condition, we get:

$$C = \ln \tan h \alpha [(f_0 - f_\infty)/2] \quad (12)$$

By substituting Eq. (12) into (11), we can obtain the theoretical equation of stress relaxation simply as

$$f_T = f_\infty + \frac{2}{\alpha} \tan h^{-1} [\alpha (f_0 - f_\infty)/2] \exp\left(-\frac{\alpha G_1}{\beta} t\right) \quad (13)$$

## Experimental

**Materials.** The materials used in this study are undrawn poly (ethylene terephthalate) monofilament fibers manufactured by Cheil Synthetic Textile Co. Inc., Gumi, Korea and drawn PET multifilament fibers (VISCOSINSSE, Swiss). The finenesses of undrawn PET monofilament fiber and drawn PET multifilament fiber were 220 denier, 1100 denier/192 filament/zero twist, respectively. The degrees of crystallinity and the orientation factors of crystalline region ( $f_c$ ) were determined from X-ray diffraction by T. Kunugi *et al.*<sup>11</sup>. X-ray diffraction pattern of ordinary PET mono- and multifila-

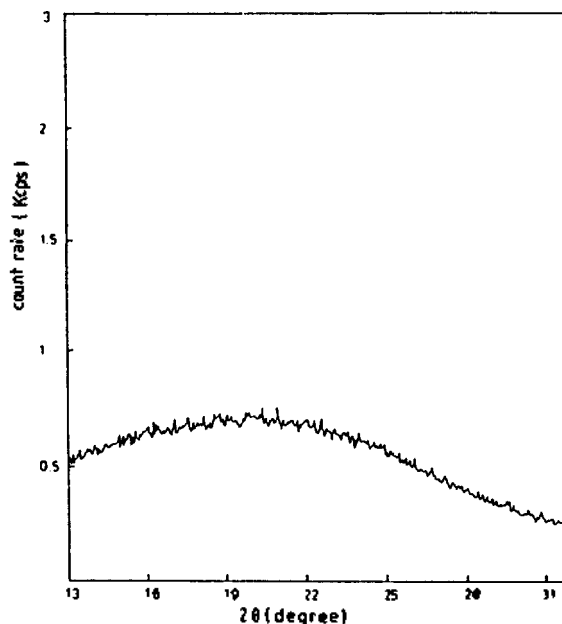


Figure 1. X-ray diffraction pattern of ordinary PET monofilament fiber.

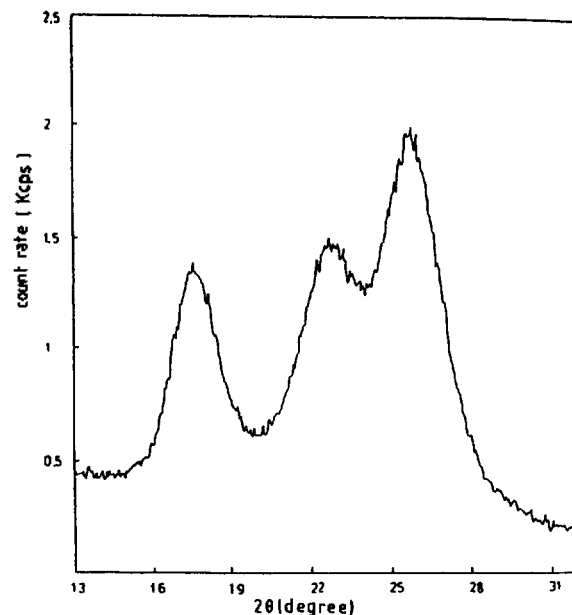
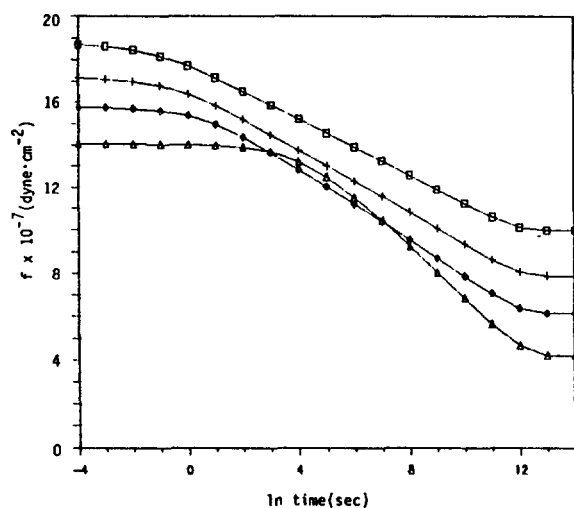


Figure 2. X-ray diffraction pattern of ordinary PET multifilament fiber.

ment fibers were shown in Figure 1 and 2, respectively. The degrees of crystallinity of PET monofiber and PET multifiber were about 10.77%, 62.11%, respectively. The orientation factor ( $f_c$ ) of PET multifilament fiber was calculated as 0.82. As shown in Figure 1, mono fiber's X-ray diffraction pattern does not clearly determine the count rate peak for calculating the orientation factor.

Fiber samples were stored in each media at constant temperature (10°C, 20°C, 30°C and 40°C) for at least 1 hour prior to their experiments.

**Stress-Relaxation Measurements.** The measurements of stress relaxation were conducted using an Instron (Toyo



**Figure 3.** Stress relaxation curves of PET monofilament fiber in  $H_2O$  of  $10^\circ C$  ( $\square$ ),  $20^\circ C$  ( $+$ ),  $30^\circ C$  ( $\diamond$ ) and  $40^\circ C$  ( $\triangle$ ). (Experimental:  $\square$ ,  $+$ ,  $\diamond$ ,  $\triangle$ , Theoretical curves:  $-$ ).

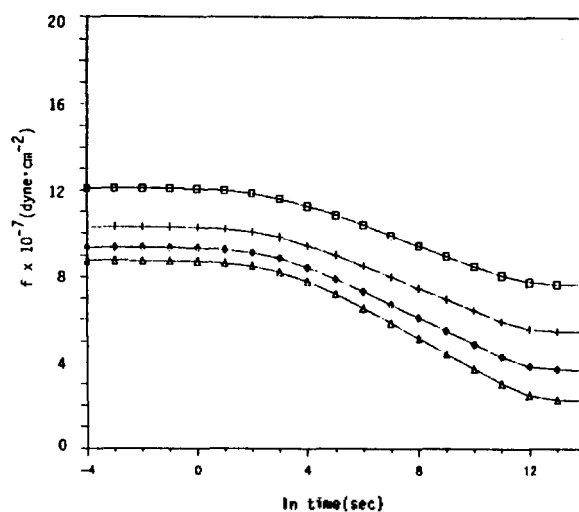


**Figure 5.** Stress relaxation curves of PET monofilament fiber in 50% DMF  $10^\circ C$  ( $\square$ ),  $20^\circ C$  ( $+$ ),  $30^\circ C$  ( $\diamond$ ) and  $40^\circ C$  ( $\triangle$ ). (Experimental:  $\square$ ,  $+$ ,  $\diamond$ ,  $\triangle$ , Theoretical curves:  $-$ ).

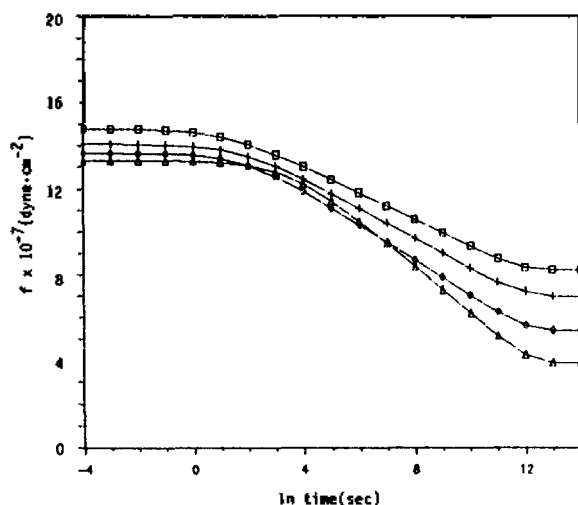


**Figure 4.** Stress relaxation curves of PET monofilament fiber in 0.05% NaOH of  $10^\circ C$  ( $\square$ ),  $20^\circ C$  ( $+$ ),  $30^\circ C$  ( $\diamond$ ) and  $40^\circ C$  ( $\triangle$ ). (Experimental:  $\square$ ,  $+$ ,  $\diamond$ ,  $\triangle$ , Theoretical curves:  $-$ ).

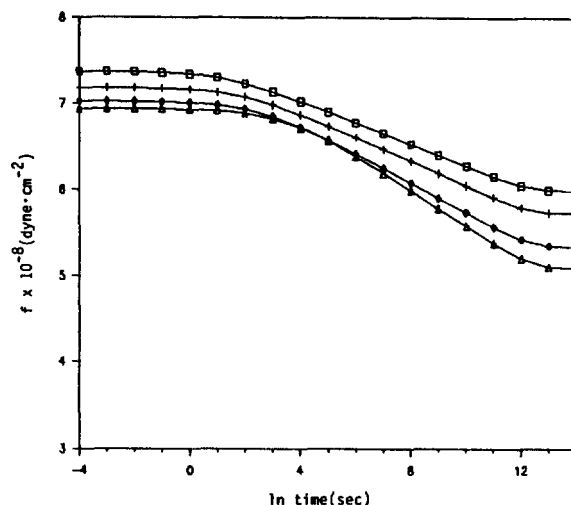


**Figure 6.** Stress relaxation curves of PET multifilament fiber in  $H_2O$  of  $10^\circ C$  ( $\square$ ),  $20^\circ C$  ( $+$ ),  $30^\circ C$  ( $\diamond$ ) and  $40^\circ C$  ( $\triangle$ ). (Experimental:  $\square$ ,  $+$ ,  $\diamond$ ,  $\triangle$ , Theoretical curves:  $-$ ).

Baldwin Co., Universal Testion Mashine, UTM-4-100 Tension). In attempt to research of solvent effects we made the solvent chamber and connected it to the low jaw of Instron. The solvent chamber was equipped with a water bath which could be kept at a desired temperature by automatic system (Julabo F20), and the water bath was thermostatically controlled within  $\pm 0.05^\circ C$ .

Stress relaxation was measured in the distilled water, 0.05 % NaOH aqueous solution and 50% DMF aqueous solution at various temperatures of  $10^\circ C$ ,  $20^\circ C$ ,  $30^\circ C$  and  $40^\circ C$ . The initial gauge length was 40 mm. Samples of 40 mm were extended rapidly at a crosshead speed of 5 mm/min to an elongation of 10% for monofilament fiber and 5% for multifilament fiber. Constant strain was maintained for more than 1800 sec. The changing values of stress were recorded on a moving chart.

## Result

**Experimental Result.** The stress relaxation curves of PET filament fibers in solvents of various temperatures are shown in Figure 3-8. As shown in figures, the stress decays gradually to equilibrium value,  $f_e$ , with time at a constant strain. The quantity,  $f_e$ , is defined as at the stress  $t = \infty$ . Then final stress,  $f_e$  is obtained by extrapolating the straight line portion of the  $f$  vs.  $1/t$  to zero.

The stress at a given time decreases with increasing temperature. 50% DMF aqueous solution has given the strongest reaction to decrease of the stress compared to 0.05% NaOH aqueous solution and water. From this experimental results, it can be seen that the flow of crystallites in amorphous region, which take part in raising the relaxation modulus<sup>12</sup>, increase with temperature and solvation. The stress relaxation has enhanced by the media in order of 50% DMF, 0.05% NaOH aqueous solution and distilled water as shown in Table 1, 2 and 5.

In Figure 3 and 4, the relaxation curves for  $40^\circ C$  show

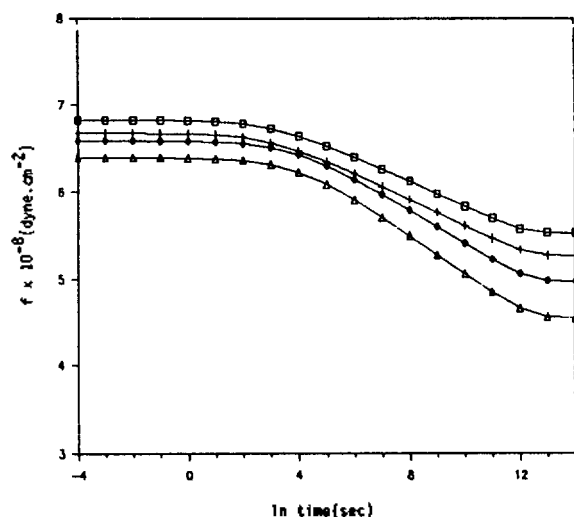


**Figure 7.** Stress relaxation curves of PET multifilament fiber in 0.05% NaOH of 10°C ( $\square$ ), 20°C ( $+$ ), 30°C ( $\diamond$ ) and 40°C ( $\triangle$ ). (Experimental:  $\square$ ,  $+$ ,  $\diamond$ ,  $\triangle$ , Theoretical curves: —).

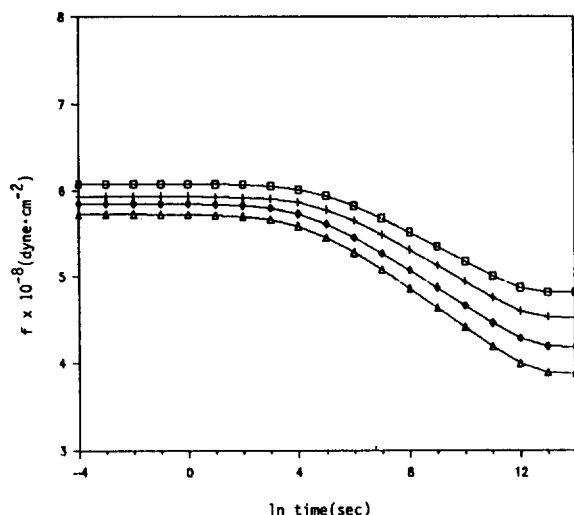


**Figure 8.** Stress relaxation curves of PET multifilament fiber in 50% DMF of 10°C ( $\square$ ), 20°C ( $+$ ), 30°C ( $\diamond$ ) and 40°C ( $\triangle$ ). (Experimental:  $\square$ ,  $+$ ,  $\diamond$ ,  $\triangle$ , Theoretical curves: —).

low slope at short times, but high slope at longer times. That is because the flow segments having shorter relaxation times than  $\ln 4$  sec had been flowed by thermal energy even when no external forces are acting. These phenomenon are higher in PET monofilament fiber of low crystallinity than PET multifilament fiber of high crystallinity as shown in Figure 3 and 4.

**Parameters for Three Element Model.** In order to establish a connection between the molecular fine structure and the mechanical properties of PET filament fiber, we applied experimental data to the theoretical stress relaxation equation, Eq. (13). Parameters  $\alpha$ ,  $\beta$ ,  $G_1$  and  $G_2$  of non-newtonian three element model were obtained by following method.

In extrapolating the straight line portion of the  $f$  vs.  $1/t$  to zero, the intercept is  $f_0$ , which equals  $G_2Sc$  at  $t = \infty$ . From the final stress  $f_t = G_2Sc$  and the initial stress

**Table 1.** The Values of  $G_1$ ,  $G_2$ ,  $\alpha$  and  $\beta$  of PET Monofilament Fibers in Various Solvents

Temp. (°C)	Solvents			
	Parameter	H <sub>2</sub> O	NaOH (0.05%)	DMF (50%)
10	$G_1 \cdot 10^{-6}$	8.741	6.549	4.446
	$G_2 \cdot 10^{-8}$	9.989	8.210	7.648
	$\alpha \cdot 10^7$	1.501	1.618	2.107
	$\beta \cdot 10^{-4}$	7.137	6.654	6.538
20	$G_1 \cdot 10^{-8}$	9.289	7.086	-4.853
	$G_2 \cdot 10^{-8}$	7.882	6.961	5.448
	$\alpha \cdot 10^7$	1.335	1.429	1.908
	$\beta \cdot 10^{-4}$	7.802	7.189	7.036
30	$G_1 \cdot 10^{-8}$	9.630	8.226	5.697
	$G_2 \cdot 10^{-8}$	6.134	5.401	3.668
	$\alpha \cdot 10^7$	1.196	1.220	1.617
	$\beta \cdot 10^{-4}$	8.593	8.041	7.514
40	$G_1 \cdot 10^{-8}$	10.380	9.381	6.485
	$G_2 \cdot 10^{-8}$	4.204	3.886	2.255
	$\alpha \cdot 10^7$	0.826	0.921	1.406
	$\beta \cdot 10^{-4}$	9.720	9.187	8.451

$G_1, G_2$ : dyne/cm<sup>2</sup>,  $\alpha$ : cm<sup>2</sup>/dyne,  $\beta$ : sec.

**Table 2.** The Values of  $G_1$ ,  $G_2$ ,  $\alpha$  and  $\beta$  of PET Multifilament Fibers in Various Solvent

Temp. (°C)	Solvents			
	Parameter	H <sub>2</sub> O	NaOH (0.05%)	DMF (50%)
10	$G_1 \cdot 10^{-8}$	26.761	26.014	25.152
	$G_2 \cdot 10^{-8}$	119.683	110.408	96.277
	$\alpha \cdot 10^7$	0.783	0.804	0.921
	$\beta \cdot 10^{-4}$	10.023	9.043	8.626
20	$G_1 \cdot 10^{-8}$	29.234	28.600	28.156
	$G_2 \cdot 10^{-8}$	114.485	105.284	90.477
	$\alpha \cdot 10^7$	0.715	0.748	0.854
	$\beta \cdot 10^{-4}$	10.742	10.237	9.864
30	$G_1 \cdot 10^{-8}$	33.824	32.462	31.672
	$G_2 \cdot 10^{-8}$	106.729	99.212	83.622
	$\alpha \cdot 10^7$	0.587	0.674	0.798
	$\beta \cdot 10^{-4}$	11.364	11.304	11.215
40	$G_1 \cdot 10^{-8}$	37.001	36.378	35.247
	$G_2 \cdot 10^{-8}$	101.762	90.808	77.573
	$\alpha \cdot 10^7$	0.493	0.586	0.728
	$\beta \cdot 10^{-4}$	12.374	12.111	12.058

$G_1, G_2$ : dyne/cm<sup>2</sup>,  $\alpha$ : cm<sup>2</sup>/dyne,  $\beta$ : sec.

$f_0 = (G_1 + G_2)Sc$ , we can obtain the parameters of spring constant  $G_1$  and  $G_2$ . In the condition of  $0 < \tan h[\alpha(f_0 - f_t)/2] < 1$ , changing the value of  $\tan h[\alpha(f_0 - f_t)/2]$  from 0 to 1, we obtained parameters of  $\alpha$  and  $\beta$  which fit best to the experimental curves. For this procedure, authors developed software program to find the value of  $\alpha$  and  $\beta$ . The determined parameters  $G_1$ ,  $G_2$ ,  $\alpha$  and  $\beta$  are relaxation time,  $\beta$ , increase with increasing temperature. But the strain modulus,  $\alpha$ , and sp-

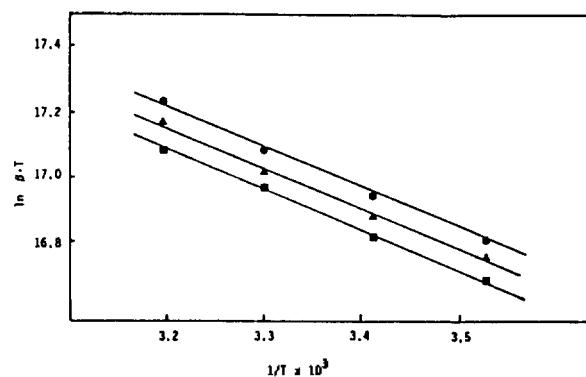


**Figure 9.** Plots of  $\ln \beta \cdot T$  vs.  $1/T$  for PET monofilament fiber in  $\text{H}_2\text{O}$  (●), 0.05% NaOH (▲) and 50% DMF aqueous solution (■).

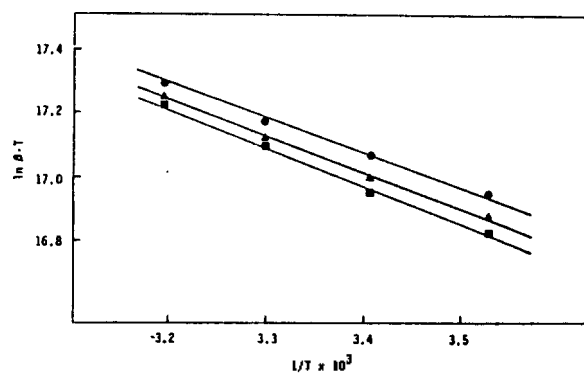


**Figure 10.** Plots of  $\ln \beta \cdot T$  vs.  $1/T$  for PET multifilament fiber in  $\text{H}_2\text{O}$  (●), 0.05% NaOH (◇) and 50% DMF aqueous solution (■).

ring constant of Maxwell element,  $G_2$ , decrease with increasing temperature. The parameters,  $G_1$ ,  $G_2$  and  $\beta$ , decrease with increasing solvent swelling effect. But the parameter,  $\alpha$ , increases with increasing swelling effect of solvent. The parameters,  $G_1$ ,  $G_2$  and  $\beta$ , increase with increasing crystallinity of PET filament fibers, but the parameter,  $\alpha$ , decreases. The experimental curves and theoretical curves agree very well.

The theoretical relaxation curves as shown in Figure 3-8 obtained by applying the stress relaxation Eq. (13) to the experimental curves will be useful to calculate the relaxation spectrum and the molecular weight distribution of PET filament fibers.

**Thermodynamic Parameters for Flow.** In Eq. (13),  $1/\beta$  is represented by the following equation.

$$1/\beta = 2\lambda k/\lambda_1 = (2\lambda/\lambda_1)(kT/h)\exp(-\Delta G^*/RT) \quad (14)$$

Thus, one obtain the following form:

$$\begin{aligned} \ln \beta \cdot T &= \Delta G^*/RT + \ln(\lambda_1/2\lambda)(h/k) \\ &= (\Delta H^*/R) 1/T - \Delta S^*/R + \ln(\lambda_1/2\lambda)(h/k) \end{aligned} \quad (15)$$

From the crystallite size of PET filament fibers determined by X-ray diffraction<sup>11</sup>, the values of  $\lambda_1$ ,  $\lambda_2$  and  $\lambda_3$  were obtained. The values of  $\lambda_2$  and  $\lambda_3$  were substituted into Eq. (16), and  $\lambda$  was calculated.

Values of  $\lambda$  is about 20 Å for undrawn monofilament fiber and 1.8 Å for drawn multifilament fiber. From the values

**Table 3.** Activation Enthalpies, Entropies and Free Energies in PET Monofilament Fibers

Solvents	Activation Enthalpy $\Delta H^*$ (Kcal/mole)	Activation Entropy $\Delta S^*$ (cal/mole · K)	Activation Free Energy $\Delta G^*$ (Kcal/mole)
$\text{H}_2\text{O}$	-2.392	-94.756	25.845
NaOH (0.05%)	-2.486	-94.937	25.805
DMF (50%)	-2.531	-95.043	25.792

**Table 4.** Activation Enthalpies, Entropies and Free Energies of Flow in PET Multifilament Fibers

solvents	Activation Enthalpy $\Delta H^*$ (Kcal/mole)	Activation Entropy $\Delta S^*$ (cal/mole · K)	Activation Free Energy $\Delta G^*$ (Kcal/mole)
$\text{H}_2\text{O}$	-1.800	-92.167	25.666
NaOH (0.05%)	-2.316	-93.810	25.639
DMF (50%)	-2.700	-95.064	25.629

**Table 5.** The  $\lambda$  Values of PET Filament Fibers in Various Solvents at 20°C

Sample	Solvent	$\text{H}_2\text{O}$	NaOH (0.05%)	DMF (50%)
Monofilament fiber		17.207	18.507	24.711
Multifilament fiber		1.720	1.800	2.055

hole distance,  $\lambda$ : Å.

of relaxation time,  $\beta$ , depending upon temperature in Table 1 and 2,  $\ln \beta \cdot T$  vs.  $1/T$  was plotted to get Figure 9 and 10. The values of thermodynamic parameters,  $\Delta G^*$ ,  $\Delta H^*$  and  $\Delta S^*$ , were obtained by the slope and intercept of the straight line in Figure 9 and 10, and summarized in Table 3 and 4. A low negative activation heat a high negative activation entropy are found in PET filament fibers. The low negative activation heat show that the relaxation phenomena of PET filament fibers is exothermic process. It is common to have negative activation entropies in relaxation and flow phenomena. Thus, it may be concluded that relaxation in PET is due to relaxation of entangled flow segments. The activation free energies for these samples are about 25.7 kcal/mol in average.

## Discussion

**Shear Volume and Crystallite Size.** In Ree-Eyring's generalized viscosity equation, parameter,  $\alpha$ , is given by:

$$\alpha = \lambda_2 \lambda_3 / 2kT = \lambda_4 / 2kT \quad (16)$$

**Table 6.** The Values of Diffusion Coefficient in Various Solvents at 20°C

Sample	Solvent	H <sub>2</sub> O	NaOH (0.05%)	DMF (50%)
Monofilament fiber		2.210 × 10 <sup>-23</sup>	2.534 × 10 <sup>-23</sup>	3.457 × 10 <sup>-23</sup>
Multifilament fiber		1.585 × 10 <sup>-25</sup>	1.740 × 10 <sup>-25</sup>	2.062 × 10 <sup>-25</sup>

diffusion coefficient,  $D$ : m<sup>2</sup>s<sup>-1</sup>.

where,  $\lambda_s$  is shear volume. We can obtain the values of  $\lambda_2$  and  $\lambda_3$  from the calculated crystallite size and the value of parameter,  $\alpha$ , obtained from experimental results. Introducing this values into Eq. (16), hole distance,  $\lambda$ , was obtained and summarized in Table 5.

The crystallite size is calculated by following method. The half-width,  $B$ , of the (010) and (100) scans were to obtain the crystal size from following equation<sup>13</sup>:

$$u = (0.89\lambda_c) / (B \cos \theta_{hkl}) \quad (5)$$

where  $\lambda_c$  is the wavelength of the X-ray,  $u$  is the crystal dimension perpendicular to the ( $h$   $k$   $l$ ) plane, and  $B_{hkl}$  is Bragg angle for this plane. The values of crystallite size obtained from (010) reflection are 25.2 Å and 58.3 Å for PET monofilament fiber and multifilament fiber, respectively.

**Diffusion and Effect of Solvents.** From the theory of absolute reaction rates, Eyring, Powell and Roseveare derived following diffusion equation<sup>10</sup>:

$$D = \lambda^2 k' x_l \quad (18)$$

Here,  $D$  represents the diffusion coefficient.

In generalized viscosity formula, viscosity is given by following equation:

$$\eta = \lambda_1 f [2\lambda k' \sin h(\lambda_2 \lambda_3 \lambda / 2kT)] \quad (19)$$

Now for ordinary viscous flow  $f \lambda_2 \lambda_3 \lambda \ll kT$  so that expanding the exponentials and keeping terms only up to the first power we have after cancelation

$$\eta = \lambda_1 k' T (\lambda_2 \lambda_3 \lambda k')^{-1} \quad (20)$$

On the other hand for molecules of the same size where Eq. (18) and (20) apply we obtain:

$$D = (\lambda_1 k' T) / (\lambda_2 \lambda_3 \eta) \quad (21)$$

By substituting Eq. (14) and (16) into Eq. (20) we can obtain the well-known viscosity formula<sup>14</sup> (Glasston, Laidler and Eyring):

$$\eta = \beta / \alpha = (k' T / \lambda^2 k') (\lambda_1 / \lambda_2 \lambda_3) \quad (22)$$

Substituting from Eq. (21) and (22) we have the equation for the self diffusion coefficient:

$$D = \lambda_1 k' T \alpha / \lambda_2 \lambda_3 \beta \quad (23)$$

Eq. (23) was applied to study the self diffusion of the flow segments of PET filament fibers in various solvents, and the self diffusion coefficients are obtained and summarized in Table 6. The orders of self diffusion coefficients in this Table 6 are similar to the orders of diffusion coefficients of PET fibers obtained by Patterson and Sheldon<sup>15</sup>.

It is a well-known fact that the swelling and the diffusion of the high polymeric fibers in good solvents are higher than those in poor solvents. From the values of diffusion coefficient of PET filament fibers, we can find that 50% DMF is more good solvent than 0.05% aqueous NaOH or distilled H<sub>2</sub>O. The values of  $D$  and  $\lambda$  for 50% aqueous DMF solvent are higher than the values for distilled water and 0.05% aqueous NaOH solvent as Table 5 and 6 show.

One see from this table that the swelling and the self diffusion of flow segments in amorphous region increase with increasing the effect of good solvent. The diffusion coefficient is determined to a certain extent by the mobilities of flow segments. Therefore, the decrease in diffusion rate are to be expected if chain mobility is restricted, for example, in case of cross-linking.

## References

- G. Halsey, H. J. White, and H. Eyring, *Text. Res. J.*, **15**(9), 295 (1945).
- T. Ree and H. Eyring, *J. Appl. Phys.*, **26**(7), 793 (1955).
- R. Meredith, *J. Text. Inst.*, **45**, 438 (1954).
- T. Ree, S. J. Hahn, and H. Eyring, *International Wool Textile Res. Conference Reprint* (1955).
- J. M. Hawthorne, *J. Appl. Polym. Sci.*, **26**, 3317 (1981).
- R. Meredith and B. S. Hsu, *J. Polym. Sci.*, **61**, 253 (1962).
- E. Passaglia and H. P. Koppehele, *J. Polym. Sci.*, **33**, 281 (1958).
- Akron Ohio, *J. Polym. Sci.*, **33**, 126 (1958).
- I. M. Ward, *Text. Res. J.*, **31**, 650 (1961).
- H. Eyring, *J. Chem. Phys.*, **4**, 283 (1936).
- T. Kunugi, I. Isobe, and K. Kimura, *J. Appl. Polym. Sci.*, **24**, 923 (1979).
- V. B. Gupta, C. Ramesh, and A. K. Gupta, *J. Appl. Polym. Sci.*, **29**, 4203 (1984).
- V. B. Gupta and S. Kumar, *J. Appl. Polym. Sci.*, **26**, 1865 (1981).
- T. Ree H. Eyring, *Reprinted from International Wool Text. Res. Conference*, **3**, 277 (1955).
- J. Crank and G. S. Park, *Diffusion in Polymers*, p. 362 (1975).